Earthquake scaling characteristics and the scale-(in)dependence of seismic energy-to-moment ratio: Insights from KiK-net data in Japan

Adrien Oth,[1] Dino Bindi,[2] Stefano Parolai,[3] and Domenico Di Giacomo[3,4]

Received 2 July 2010; revised 17 August 2010; accepted 23 August 2010; published 8 October 2010.

[1] We investigate earthquake source characteristics and scaling properties using the results of a spectral inversion of more than 29,000 accelerometric borehole recordings from 1,826 earthquakes (M_{JMA} 2.7–8) throughout Japan. We find that the calculated source spectra can be well characterized by the omega-square model and show on average self-similar scaling over the entire magnitude range, with median stress drops of 1.1 and 9.2 MPa for crustal and subcrustal events, respectively. The seismic energy-to-moment ratio, as theoretically expected if the omega-square model is valid, shows a strong dependency on stress drop only, which, in conjunction with data selection practice in some studies to cope with limited recording bandwidth, can explain the often observed apparent scale-dependence. Our observations suggest that there is no significant deviation from similarity of the energy radiation in the investigated magnitude range and that the observed scatter is mainly related to the scatter in stress drop. **Citation:** Oth, A., D. Bindi, S. Parolai, and D. Di Giacomo (2010), Earthquake scaling characteristics and the scale-(in)dependence of seismic energy-to-moment ratio: Insights from KiK-net data in Japan, *Geophys. Res. Lett.*, *37*, L19304, doi:10.1029/2010GL044572.

1. Introduction

[2] Amongst the most fundamental and, at the same time, most heavily debated topics in modern seismology, the question in how far earthquake source parameters scale with earthquake size is of prime importance, since it has significant implications for seismic hazard assessment. In particular, the energy radiated during seismic faulting is of highest interest since it directly reflects the dynamic characteristics of the rupture process [e.g., *Kanamori and Rivera*, 2004]. Consequently, a scale-dependency of the seismic energy-to-moment ratio (also termed as scaled energy) $\tilde{e} = E_R / M_0$ would imply that the rupture dynamics of small and large earthquakes differ [e.g., *Kanamori and Heaton*, 2000], a finding that in turn would have profound implications both for our understanding of the physics of earthquakes and strong ground motion prediction.

[3] Yet a fundamental controversy still exists upon the scaling characteristics of seismic energy-to-moment ratio. Over the past two decades, a significant number of studies provided persuasive evidence for an increase of $\tilde{e}$ with moment [e.g., *Abercrombie*, 1995; *Mayeda and Walter*, 1996; *Izutani and Kanamori*, 2001; *Mori et al.*, 2003; *Mayeda et al.*, 2005, 2007; *Takahashi et al.*, 2005], sometimes even in conjunction with self-similar static scaling (i.e., $M_0 \propto f_C^{-3}$, f_C being the corner frequency).

[4] In contrast, other studies cast doubt on these findings. *Ide and Beroza* [2001] and *Ide et al.* [2003] suggested that the often-observed scale-dependency of $\tilde{e}$ may be due to a systematic underestimation of energy resulting from limited recording bandwidth and too simple attenuation corrections. *Prieto et al.* [2004] found compelling evidence for approximately constant apparent stress and most recently, *Baltay et al.* [2010] came to the same conclusion from the analysis of seismic coda of four earthquake sequences in western North America.

[5] Thus the issue of whether or not $\tilde{e}$ is scale-dependent and how it is related to the scaling characteristics of other source parameters remains elusive. In order to obtain new insights on these issues, we use source spectra of a large set of earthquakes in Japan recorded by the KiK-net network [e.g., *Okada et al.*, 2004], obtained from spectral inversion of S-waves, and we investigate the relation between energy-to-moment ratio and stress drop and in how far specifically the former is scale-dependent.

2. Data and Analysis

[6] We applied a non-parametric inversion scheme to separate the Fourier amplitude spectra of S-waves into source spectra, attenuation characteristics and site response, similar to the original works of *Andrews* [1986] and *Castro et al.* [1990]. In this approach, the functional form of the attenuation operator is not pre-defined, thus providing a means for reliable attenuation correction without strong a-priori assumptions. The attenuation-corrected spectra were separated into their source and site contributions, setting the average site response of all borehole sensors to unity. A bootstrap analysis of 100 consecutive inversions indicates that the technique provides highly stable results. The details of the data processing and inversion methodology are given by A. Oth et al. (Spectral analysis of K- and KiK-net data in Japan: II. On attenuation characteristics, source spectra and site response of borehole and surface stations, submitted to *Bulletin of the Seismological Society of America*, 2010).

[1]European Center for Geodynamics and Seismology, Walferdange, Luxembourg.
[2]Center for Disaster Management and Risk Reduction Technology, Helmholtz Centre Postdam, GFZ German Research Centre for Geosciences, Potsdam, Germany.
[3]Earthquake Risk and Early Warning Section, Helmholtz Centre Potsdam, GFZ German Research Centre for Geosciences, Potsdam, Germany.
[4]Now at International Seismological Centre, Thatcham, UK.

0094-8276/10/2010GL044572

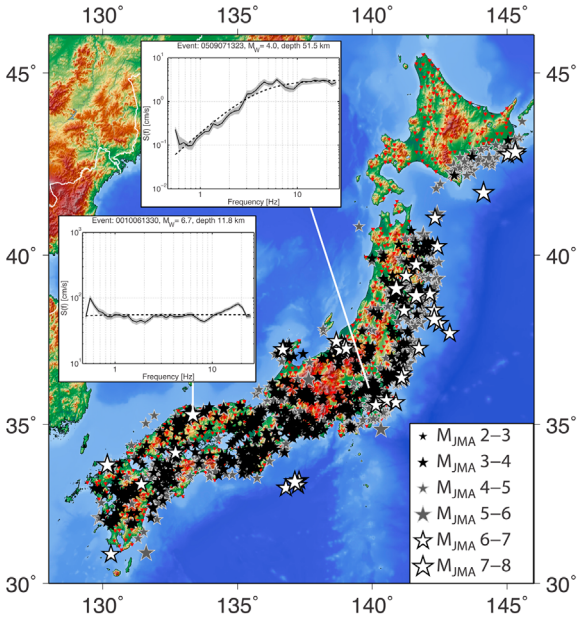

Figure 1. Map of the study area showing the epicenters (stars) of earthquakes and stations (inverse red triangles) used in this work. Two examples of source spectra (at 5 km reference distance) are depicted as insets. For each of these, the solid black line indicates the average from inversion of 100 bootstrap samples while the gray-shaded area indicates the standard deviation. The dashed line represents the best-fitting ω^2 source model.

[7] The analysis below is based on a dataset of more than 29,000 borehole recordings from 1,826 earthquakes obtained at 637 stations and covering a hypocentral distance range of 5–250 km and a magnitude range of M_{JMA} 2.7–8 (Figure 1). In the following, we refer to events with hypocentral depth $d_{hyp} \leq 30$ km and $d_{hyp} > 30$ km as crustal and subcrustal, respectively. We only considered events and stations with at least 3 available recordings, but for the vast majority, more than 6 and in most cases also far more than 10 or 20 records were available. Therefore, directivity and radiation pattern effects are effectively averaged out.

[8] Assuming an ω^n source model, the acceleration source spectra can be written as:

$$S(f) = (2\pi f)^2 \frac{R^{\theta\varphi} VF}{4\pi\rho v_S^3 R_0} M(f), \qquad \text{with} \qquad M(f) = \frac{M_0}{1 + (f/f_c)^n}, \tag{1}$$

where $R^{\theta\varphi}$ represents the average radiation pattern of S-waves set to 0.55 [*Boore and Boatwright*, 1984], $R_0 = 5$ km is the reference distance, $V = 1/\sqrt{2}$ accounts for the separation of S-wave energy onto two horizontal components, $F = 2$ is the free surface factor and ρ and v_S are the density and shear wave velocity in the source region. For the latter, we used $\rho = 2.8$ g/cm^3, $v_S = 3.5$ km/s and $\rho = 3.6$ g/cm^3, $v_S = 4.2$ km/s for crustal and subcrustal events respectively. Finally, n determines the high-frequency fall-off of the source spectrum.

[9] Setting $n = 2$ leads to the well-known ω^2 model [*Aki*, 1967; *Brune*, 1970, 1971], which is generally considered to provide an appropriate representation of the source spectrum of small and moderate earthquakes [e.g., *Izutani and Kanamori*, 2001]. Since the inverted acceleration source spectra show an increase approximately proportional to f^2 at low frequencies and a plateau at high frequencies (which is only the case if $n = 2$), we use $n = 2$ and fit equation (1) to the inverted spectra using non-linear least-squares to determine M_0 (respectively moment magnitude M_W [*Hanks and Kanamori*, 1979]) and f_C. For large events with $M_{JMA} \geq 5$, where f_C is likely to be smaller than the lowest frequency in our analysis, we constrained M_0 to the value given in the GCMT catalogue (www.globalcmt.org). Two examples of the source spectra are shown in Figure 1, with the best fitting ω^2 source spectrum indicated as dashed line, showing good agreement between observed and fitted spectra.

[10] Stress drop estimates $\Delta\sigma$ are computed following *Hanks and Thatcher* [1972]:

$$\Delta\sigma = 8.5 M_0 \left(\frac{f_c}{v_S}\right)^3, \tag{2}$$

and we calculate the radiated energy E_R from the inverted S-wave source spectra as [e.g., *Izutani and Kanamori*, 2001] (neglecting the contribution of P-waves, compare also with equation (1)):

$$E_R = \frac{4\pi}{5\rho v_S^5} \int_0^\infty |Cf^{-1}S(f)|^2 df, \qquad \text{with} \qquad C = \frac{\rho v_S^3 R_0}{\pi R^{\theta\varphi} VF}. \tag{3}$$

3. M_{JMA} – M_W Scaling

[12] *Fukushima* [1996], starting from the assumption that M_{JMA} can be considered to result from peak horizontal displacement at 5 seconds period and that the ω^2 model holds, derived a relationship between seismic moment and M_{JMA} (in the M_{JMA} range ~4–8, similar to our dataset) of the form $\log_{10}(M_0^{-1} + 10^{-17} M_0^{-1/3}) = C_1 \cdot M_{JMA} + C_2$, where M_0 is given in dyn·cm. Figure 2a shows the determined moment magnitudes M_W versus M_{JMA}. At first glance, a linear relationship seems to hold between M_{JMA} and M_W, and the relation of *Fukushima* [1996] does not provide an appropriate description for earthquakes smaller than about M_{JMA} 4.5–5 (Fukushima's dataset contained however predominantly events with M_{JMA} in the range 5–8). We performed a linear orthogonal regression to determine the optimal linear fit and, accounting for potential saturation effects of M_{JMA} (however not noticeable from Figure 2a by eye), a nonlinear least squares regression including a quadratic term (Table 1). Both the linear and quadratic fits provide comparable overall rms residuals of 0.22 and 0.21 magnitude units, respectively. However, for small events ($M_{JMA} \approx$ 2.7–3.5), the linear fit systematically underestimates M_W (rms residual 0.24), and the quadratic fit provides better estimates of M_W in that M_{JMA} range (rms residual 0.19), while the opposite is true for large M_{JMA}. An F test between the linear and quadratic models provides statistical evidence that over the entire M_{JMA} range, the quadratic fit can be considered more appropriate.

4. Stress Drops and Static Scaling Relationship

[13] If the principle of self-similarity holds between small and large earthquakes, then the well-known scaling relation

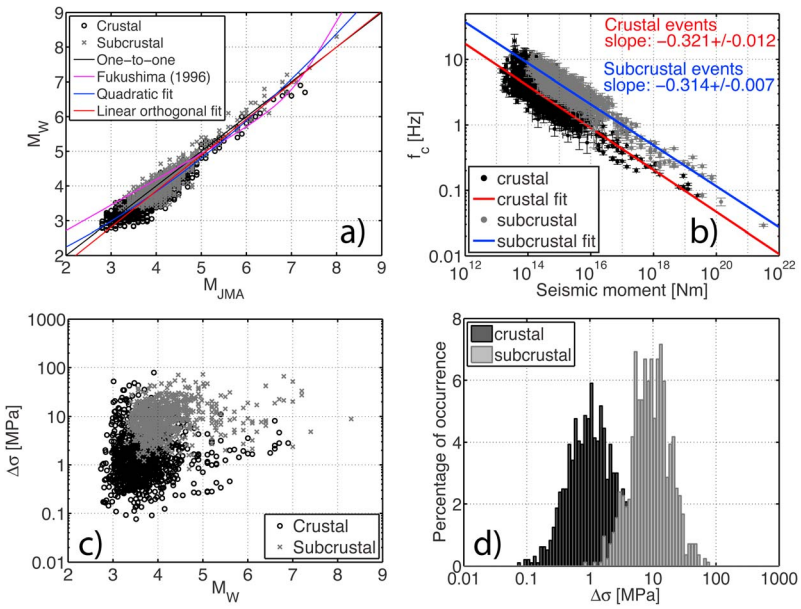

Figure 2. (a) M_W as derived from source spectral fitting versus M_{JMA} as provided by the KiK-net database. Blue and red lines: quadratic and linear fits with parameters given in Table 1. The magenta line represents the relationship of *Fukushima* [1996]. (b) f_C vs. M_0 for crustal and subcrustal earthquakes. The slope error estimates represent the 95% confidence bounds. (c) Stress drop $\Delta\sigma$ versus M_W. (d) Histograms depicting the stress drop distribution.

$M_0 \propto f_C^{-3}$ is expected to apply [*Aki*, 1967]. Figure 2b shows log f_C versus log M_0 for crustal (black dots, red line) and subcrustal events (gray dots, blue line). The slopes are in both cases very close to the expected value of −1/3. Considering a potential modification of the scaling relationship to $M_0 \propto f_C^{-(3+\varepsilon)}$ [*Kanamori and Rivera*, 2004], we find $\varepsilon = 0.12 \pm 0.12$ for the crustal and $\varepsilon = 0.18 \pm 0.08$ for the subcrustal case, which is far smaller than the values of 0.5–1 reported for instance by *Mayeda et al.* [2007]. Considering the regressional errors obtained for ε, we cannot reject the null hypothesis of self-similar scaling for crustal events at 95% confidence level. The subcrustal events seem to show a more robust, but still only slight increase of $\Delta\sigma$ with M_0 (which would be consistent with the scaling interpretations of *Kanamori and Rivera* [2004]), but this deviation from self-similarity is still extraordinary small in view of other uncertainties apart from the regressional error of fit of the f_C-M_0 relation (e.g., 3D attenuation effects) that are difficult to quantify. Thus, we find no significant deviation from self-similarity over the entire analyzed magnitude range.

[14] In Figure 2c, stress drop is plotted versus M_W, and the stress drop distributions are depicted in Figure 2d. The estimates for subcrustal earthquakes are rather tightly clustered and approximately log-normally distributed (median 9.2 MPa), while in the crustal case, the distribution is broader and slightly asymmetric with a prevalence of smaller values (median 1.1 MPa). We performed a Lilliefors goodness-of-fit test of composite normality on both samples (in log-scale), and in the crustal case, the null hypothesis of normal distribution could be rejected at a significance level of 0.1%, while this was not the case for the subcrustal events, where the returned p-value (i.e., the probability, under the null hypothesis, that a value at least as extreme as observed of the test statistic is obtained) of 0.41 clearly forbids the rejection of the null hypothesis at acceptable significance level. The smaller variability in the case of subcrustal earthquakes may result from the fact that these are predominantly linked to the subduction zone (Oth et al., submitted manuscript, 2010) and thus related to a rather uniform tectonic feature, while the broader distribution for crustal earthquakes reflects the stronger heterogeneity of the crustal stress field and fault mechanisms. A two-sample K-S test rejects the null hypothesis that the crustal and subcrustal

Table 1. Functional Forms, Coefficients and RMS Residual of the Three M_W-M_{JMA}, respectively M_0-M_{JMA}, Relationships Depicted in Figure 2a

Relation	Coefficients	RMS Residual
Fukushima [1996] $\log_{10}(M_0^{-1} + 10^{-17}M_0^{1/3}) = C_1 \cdot M_{JMA} + C_2$, with M_0 in dyn·cm	$C_1 = -1.10 \pm 0.06$ $C_2 = -17.92 \pm 0.42$	0.41
Quadratic nonlinear least squares fit $M_W = C_1 \cdot M_{JMA}^2 + C_2 \cdot M_{JMA} + C_3$	$C_1 = 0.057 \pm 0.006$ $C_2 = 0.455 \pm 0.055$ $C_3 = -1.105 \pm 0.126$	0.21
Linear orthogonal least squares fit $M_W = C_1 \cdot M_{JMA} + C_2$	$C_1 = 1.037 \pm 0.008$ $C_2 = -0.297 \pm 0.034$	0.22

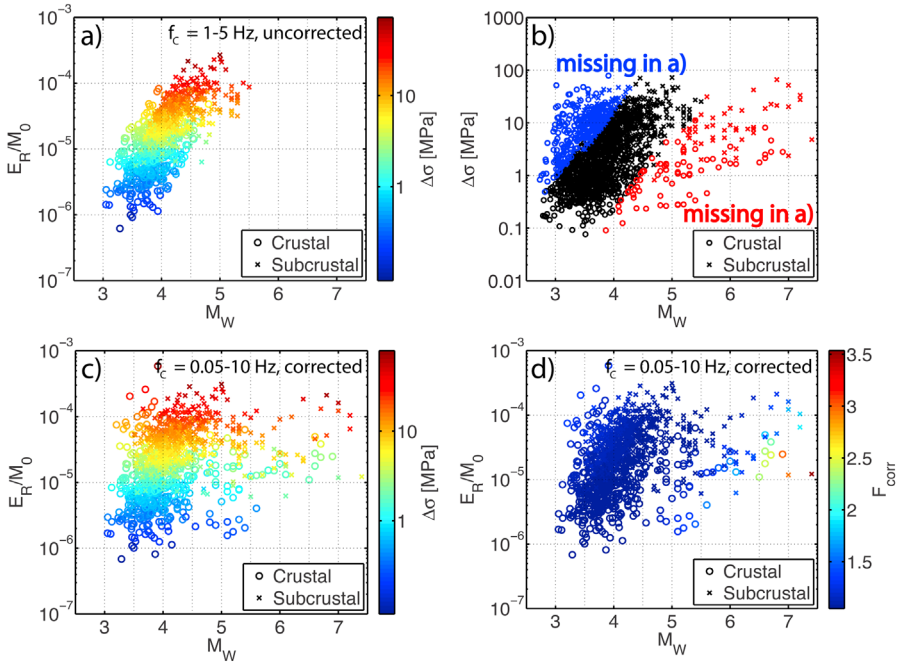

Figure 3. (a) Scaled energy $\tilde{e}$ versus M_W, using only events with f_C ranging between 1 and 5 Hz. (b) Stress drop $\Delta\sigma$ versus M_W, indicating events considered in Figure 3a as black symbols while missing events with $f_C > 5$ Hz and $f_C < 1$ Hz are marked in blue and red, respectively. (c) Scaled energy versus M_W, using events with f_C ranging between 0.05–10 Hz, color-coded with stress drop. (d) Same as Figure 3c, color-coded with respect to correction factor F_{corr}.

stress drop samples are drawn from the same distribution at a significance level of 0.1%.

5. Scale-(In)dependence of Seismic Energy-to-Moment Ratios

[15] The results presented so far hence support the validity of the self-similar static scaling relationship (i.e. $M_0 \propto f_C^{-3}$) over the entire analyzed magnitude range. Since moreover the source spectral shape is well approximated by the ω^2 model, in which case $\tilde{e} \propto M_0 f_C^3$, or following equation (2), $\tilde{e} \propto \Delta\sigma$, we would expect to see on average a constant value of scaled energy independent of moment [*Izutani and Kanamori*, 2001; *Kanamori and Rivera*, 2004], with the scatter from this average being directly related to the scatter in stress drop.

[16] A general problem in the estimation of radiated energy resides in the limited bandwidth of seismic recording systems, and in particular, limitations at high frequencies can have a serious impact on energy estimates, since more than 80% of the energy are carried by waves of higher frequency than the corner frequency [*Ide and Beroza*, 2001]. Therefore, in order to avoid an underestimation of radiated energy, some authors selected events for the calculation of scaled energy according to the values of their estimated corner frequencies with respect to the analyzed frequency band. For instance, *Abercrombie* [1995] only used events for which $2f_{min} \le f_C \le f_{max}/5$, and *Mayeda and Walter* [1996] limited their analysis to events for which at least 70% of the energy were radiated in their analyzed frequency range. As *Ide and Beroza* [2001] pointed out, selection criteria of this type are likely to introduce an artificial trend. Considering the case of a simple ω^2 source, they also proposed a simple formulation for correcting estimates of scaled energy for bandwidth limitation.

[17] With this extensive dataset at hand, we explore these issues and investigate the scaling characteristics of $\tilde{e}$. First, we follow the selection criteria used by *Abercrombie* [1995] and only consider events with $f_C = 1$–5 Hz. Figure 3a shows $\tilde{e}$ versus M_W and each data point is color-coded following its estimated stress drop. We applied no correction for missing energy, since its effect is negligible due to this rigorous selection. An apparent increase of $\tilde{e}$ with increasing M_W is immediately visible. However, the stress drop color-coding indicates that for a given stress drop level, the estimates of energy-to-moment ratio are remarkably constant, and that the increase of scaled energy is simply related to an increase of stress drop. Figure 3b shows again $\Delta\sigma$ versus M_W, where the values of discarded events in Figure 3a due to too high or too low f_C are shown as blue and red symbols, respectively. As speculated by *Ide and Beroza* [2001], the missing events roughly define a triangle in the upper left corner ($f_C > 5$ Hz), but also in the lower right corner ($f_C < 1$ Hz). This way a clear artificial scale-dependency is introduced in stress drop, which is then reflected by a scale-dependency of scaled energy as well.

[18] In Figures 3c and 3d, we used all events with estimated corner frequencies in the range 0.05–10 Hz, which represents the largest part of our dataset, and we determined correction factors F_{corr} following *Ide and Beroza* [2001]. Figure 3c shows scaled energy with stress drop color-coding, while in Figure 3d, the color-coding relates to the correction factor F_{corr}. As can be seen from Figure 3d, F_{corr} is generally lower than 1.5–2, with significant impact only for the largest earthquakes where f_C is smaller than the lowest frequency of analysis (0.5 Hz). Figure 3c clearly confirms our expectations from the fact that the source spectra obey

the ω^2 model with self-similar static scaling, i.e. that the seismic energy-to-moment ratio does not show any dependency on seismic moment. Rather, for each given stress drop level, $\tilde{e}$ is remarkably constant, and the overall scatter is only reflecting the scatter in stress drop (compare Figure 3c with Figure 3b).

6. Conclusions

[19] Our results from Japan thus indicate that the ω^2 source model provides an excellent overall description of source spectral shape and that the scaling relationship $M_0 \propto f_C^{-3}$ seems to hold over the entire investigated magnitude range. Moreover, the seismic energy-to-moment ratio does not show any significant trend with seismic moment, and the observed scatter can be fully attributed to the scatter in stress drop estimates. While the latter finding may seem trivial with respect to the first result of ω^2 source spectral behavior, it has precisely been a subject of controversial discussion over the recent years and not been shown in this clarity and using such an extensive database up to date. We also clearly demonstrated the suspicion of *Ide and Beroza* [2001] that selection procedures based on corner frequency indeed introduce artificial trends in the $\tilde{e}$ versus M_0 scaling behavior and can explain some of the scale-dependency of $\tilde{e}$ seen in earlier studies.

[20] Finally, we note that our results were obtained through analysis of earthquakes spread throughout the entirety of the Japanese archipelago, while many of the earlier studies were based on results from specific earthquake sequences respectively mainshock/aftershock analysis. Therefore, it may be possible that within a particular earthquake sequence, a deviation from self-similarity may occur, which however seems not to be the case over such a large area as Japan.

[21] **Acknowledgments.** We wish to thank the National Research Institute for Earth Science and Disaster Prevention (NIED) for making the KiK-net data available. D. Di Giacomo was supported by a research grant from the European Center for Geodynamics and Seismology and enrolled in the PhD program of the University of Potsdam, Germany. This publication was supported by the National Research Fund, Luxembourg (FNR/10/AM4/45).

References

Abercrombie, R. E. (1995), Earthquake source scaling relationships from -1 to 5 ML using seismograms recorded at 2.5-km depth, *J. Geophys. Res.*, *100*, 24,015–24,036, doi:10.1029/95JB02397.

Aki, K. (1967), Scaling law of seismic spectrum, *J. Geophys. Res.*, *72*, 1217–1231, doi:10.1029/JZ072i004p01217.

Andrews, D. J. (1986), Objective determination of source parameters and similarity of earthquakes of different size, in Earthquake Source Mechanics, edited by S. Das, J. Boatwright, and C. H. Scholz, pp. 259–268, AGU, Washington, D. C.

Baltay, A., G. Prieto, and G. C. Beroza (2010), Radiated seismic energy from coda measurements and no scaling in apparent stress with seismic moment, *J. Geophys. Res.*, *115*, B08314, doi:10.1029/2009JB006736.

Boore, D. M., and J. Boatwright (1984), Average body-wave radiation coefficients, *Bull. Seismol. Soc. Am.*, *74*, 1615–1621.

Brune, J. N. (1970), Tectonic stress and the spectra of seismic shear waves from earthquakes, *J. Geophys. Res.*, *75*, 4997–5009, doi:10.1029/JB075i026p04997.

Brune, J. N. (1971), Correction, *J. Geophys. Res.*, *76*, 5002, doi:10.1029/JB076i020p05002.

Castro, R. R., J. G. Anderson, and S. K. Singh (1990), Site response, attenuation and source spectra of S waves along the Guerrero, Mexico, subduction zone, *Bull. Seismol. Soc. Am.*, *80*, 1481–1503.

Fukushima, Y. (1996), Scaling relations for strong ground motion prediction models with M^2 terms, *Bull. Seismol. Soc. Am.*, *86*, 329–336.

Hanks, T. C., and H. Kanamori (1979), A moment magnitude scale, *J. Geophys. Res.*, *84*, 2348–2350, doi:10.1029/JB084iB05p02348.

Hanks, T. C., and W. Thatcher (1972), A graphical representation of seismic source parameters, *J. Geophys. Res.*, *77*, 4393–4405, doi:10.1029/JB077i023p04393.

Ide, S., and G. C. Beroza (2001), Does apparent stress vary with earthquake size?, *Geophys. Res. Lett.*, *28*, 3349–3352, doi:10.1029/2001GL013106.

Ide, S., G. C. Beroza, S. G. Prejean, and W. L. Ellsworth (2003), Apparent break in earthquake scaling due to path and site effects on deep borehole recordings, *J. Geophys. Res.*, *108*(B5), 2271, doi:10.1029/2001JB001617.

Izutani, Y., and H. Kanamori (2001), Scale-dependence of seismic energy-to-moment ratio for strike-slip earthquakes in Japan, *Geophys. Res. Lett.*, *28*, 4007–4010, doi:10.1029/2001GL013402.

Kanamori, H., and T. H. Heaton (2000), Microscopic and macroscopic physics of earthquakes, in Geocomplexity and the Physics of Earthquakes, *Geophys. Monogr. Ser.*, vol. 120, edited by J. Rundle, D. Turcotte, and W. Klein, pp. 147–163, AGU, Washington, D. C.

Kanamori, H., and L. Rivera (2004), Static and dynamic scaling relations for earthquakes and their implications for rupture speed and stress drop, *Bull. Seismol. Soc. Am.*, *94*, 314–319, doi:10.1785/0120030159.

Mayeda, K., and W. R. Walter (1996), Moment, energy, stress drop, and source spectra of western United States earthquakes from regional coda envelopes, *J. Geophys. Res.*, *101*, 11,195–11,208, doi:10.1029/96JB00112.

Mayeda, K., R. Gök, W. R. Walter, and A. Hofstetter (2005), Evidence for non-constant energy/moment scaling from coda-derived source spectra, *Geophys. Res. Lett.*, *32*, L10306, doi:10.1029/2005GL022405.

Mayeda, K., L. Malagnini, and W. Walter (2007), A new spectral ratio method using narrowband coda envelopes: evidence for non-self-similarity in the Hector Mine sequence, *Geophys. Res. Lett.*, *34*, L11303, doi:10.1029/2007GL030041.

Mori, J., R. E. Abercrombie, and H. Kanamori (2003), Stress drops and radiated energies of aftershocks of the 1994 Northridge, California, earthquake, *J. Geophys. Res.*, *108*(B11), 2545, doi:10.1029/2001JB000474.

Okada, Y., K. Kasahara, S. Hori, K. Obara, S. Sekiguchi, H. Fujiwara, and A. Yamamoto (2004), Recent progress of seismic observation networks in Japan-Hi-net, F-net, K-NET and KiK-net, *Earth Planets Space*, *56*, XV–XXVIII.

Prieto, G. A., P. M. Shearer, F. L. Vernon, and D. Kilb (2004), Earthquake source scaling and self-similarity estimation from stacking P and S spectra, *J. Geophys. Res.*, *109*, B08310, doi:10.1029/2004JB003084.

Takahashi, T., H. Sato, M. Ohtake, and K. Obara (2005), Scale dependence of apparent stress for earthquakes along the subducting Pacific plate in northeastern Honshu, Japan, *Bull. Seismol. Soc. Am.*, *95*, 1334–1345, doi:10.1785/0120040075.

D. Bindi, Center for Disaster Management and Risk Reduction Technology, Helmholtz Centre Potsdam, GFZ German Research Centre for Geosciences, Telegrafenberg, D-14473 Potsdam, Germany. (bindi@gfz-potsdam.de)

D. Di Giacomo, International Seismological Centre, Pipers Lane, Thatcham, RG19 4NS, UK. (domenico@isc.ac.uk)

A. Oth, European Center for Geodynamics and Seismology, 19, rue Josy Welter, L-7256 Walferdange, Luxembourg. (adrien.oth@ecgs.lu)

S. Parolai, Earthquake Risk and Early Warning Section, Helmholtz Centre Potsdam, GFZ German Research Centre for Geosciences, Telegrafenberg, D-14473 Potsdam, Germany. (parolai@gfz-potsdam.de)